10.48047/jocaaa.2024.33.08.136

Siberian Tiger Carpet Weaver Optimization based Hybrid Deep Learning for Multi-level Cotton Leaf Disease Classification under Complex Environment

[1]Vasanth Kumar Reddy G, [2]Dr. Punith Kumar M B

[1]Assistant Professor, Department of EEE,
Rajeev Institute of Technology, Hassan (Karnataka), INDIA
(Affiliated to VTU, Belagavi)
Email: rvasanthg@rithassan.ac.in

[2]Professor, Department of ECE,
P.E.S College of Engineering, Mandya,(Karnataka), INDIA
(Autonomous Institute under VTU Belagavi)
Email: punithpes@gmail.com

Abstract: In India, Cotton is the most important crops for agricultural economy but is highly susceptible to plant diseases. Any loss of this crop leads to a significant reduction in yield. There are several reasons for crop loss, especially leaf disease is the major issue. The crop loss due to leaf disease is rapidly increasing that significantly affects productivity and economic stability if it is not maintained properly. Since diseases in the crop are predictable, early detection plays a crucial role in controlling agricultural losses. Conventional manual inspection techniques are error-prone, ineffectual, and subjective; thus, it delays the treatment plan. To mitigate these issues, a hybrid optimization-based hybrid Deep Learning (DL) framework is introduced for detecting and classifying the leaf diseases named Siberian Tiger Carpet Weaver Optimization based EfficientNet_Sheperd Convolutional Neural Network (STCWO_EffNet_ShCNN). First, an image pre-processing is done utilizing Geometric Mean Filtering. The plant leaf area segmentation is carried out using Region-based Online Selective Examination (ROSE). Then, feature extraction is performed. After that, cotton leaf detection is done by EffNet_ShCNN, where its parameters are tuned by proposed STCWO. The detected disease is categorized into healthy and non-healthy. If the detected disease is non-healthy, the disease will be classified using STCWO_EffNet_ShCNN. The effectiveness of STCWO-EffNet_ShCNN is assessed through various evaluation measures like accuracy, sensitivity and specificity that achieves the values of 92.745%, 91.320% and 93.925%.

Keywords: Agriculture, Cotton leaf disease, Geometric Mean Filtering, Siberian Tiger Optimization, Carpet Weaver Optimization.

1. Introduction

For the past few years, sustainable agriculture has obtained greater interest among researchers, which includes several difficulties in agriculture, such as the plantation cycle, resources utilization and lifecycle of crops [1]. India is well known for its farming and agriculture, which is the largest economic sector and plays a significant role in the country's socio-economic development. In India, several crops are produced in diverse areas and in diverse weather conditions. Therefore, various diseases affect the plants [2]. The cultivation of crops largely depends on rainfall, soil quality, and climatic conditions, which can significantly impact yield and potentially lead to crop loss. Agriculture plays a crucial role in providing food and economic growth. So, it is important to predict the diseases in the leaf at the initial stage [3]. Cotton, which is also known as white gold is the foremost agriculture crop in India. It has a significant effect on Indian agriculture sector. Indian cotton cultivation is also damaged by various uncertainties based on crop cultivation, preservation, transportation, and warehouses. Recently, there has been a great loss in the quantity and quality of cotton yield due to diverse diseases impacting the plants [4]. As an agricultural commodity, cotton provides remarkable ability for strengthening the economic success of a nation [5]. Cotton contributes to natural fiber production holds the most significance in textile industry,

10.48047/jocaaa.2024.33.08.136

facilitating its expansion. It is also a significant crop for fiber production all over the world, which frequently experiences important risks from leaf-borne diseases [6]. Thus, implementing advanced disease detection techniques can help in early identification and control, thereby protecting crop yield and quality.

Cotton plant is easily susceptible to bacterial and viral infections that can be differentiated through the observation of its leaves [5]. These diseases can severely affect the yield and quality of crops and pose complexities for sustainable production [6]. Usually, cotton pests' management and diseases involve the use of chemical pesticides [7]. Several people rely on cotton crop for its production. Owing to the increasing domestic and global demand, cotton's productivity has currently become more significant. Farmers understand the symptoms with their own experiences, which leads to inaccurate diagnosis and control measures, like overexploitation of pesticides at inappropriate time. By enhancing the productivity and efficiency of cotton field, identifying these diseases minimizes the identification efficiency through manual process. Even though the experts utilize their own eyes for assessing symptoms, large farms need continuous expert oversight which is expensive. In order to optimize the production of crop and improve cotton's value, it is significant to effectively protect the cotton plant from diseases. [8]. Hence, an automatic technique for detecting cotton diseases is significant in large crop fields and early detection. These types of models should be designed by utilizing Machine Learning (ML), image processing, and neural network techniques. With the development of image processing techniques, the issues in these techniques should be rapidly and consistently mitigated [9]. The early phase of detection plays a significant role in efficient disease management [1]. Several researches have been performed to classify cotton leaf diseases using several pattern recognition models for detection and classification of cotton leaf diseases [5].

ML approaches have the strength or ability for early identification of different crop diseases; thus, they provide important perceptions to farmers and other stakeholders. This prominent technique enables timely interventions, which mitigates the risk of substantial losses in agricultural production [5]. These techniques mainly rely on essential features, such as color and texture to classify diseases. Furthermore, ensemble techniques demonstrated high efficiency in classification tasks. Existing models often need manual feature extraction, limiting accuracy and adaptability. Therefore, DL techniques automate this process, enhancing precision and enabling robust, real-time cotton leaf disease classification across diverse conditions. Current advancements in cotton leaf disease classification have been designed by the adoption of DL approaches, especially Convolutional Neural Networks (CNNs). These systems efficiently control spatial correlations in images for identifying and classifying the disease symptoms on cotton leaves [6]. Recently, the use of DL in neural networks is an ideal choice among researchers. DL is the most preferred choice based on the significant function of extracting features automatically from given images [1]. DL integrates image processing and data evaluation, enabling various valuable insights, especially when applied in agricultural sector. CNN, Deep Belief Network (DBN), and Recurrent Neural Network (RNN) are the few approaches to DL-based computer vision applications, which attained high accuracy [10]. Regardless of the advancements in DL and existing ML approaches, an issue remains in designing modules that balance high performance with computational efficiency, especially for real-time disease management detections on resource-constrained devices. Hence, hybrid optimization based on DL is introduced for classifying cotton leaf disease to provide efficient generalizability and feasibility.

The contribution of this research is to design a STCWO_EffNet_ShCNN for classifying cotton leaf disease. In this research, Geometric Mean Filtering is utilized for image pre-processing. Then, ROSE is utilized to segment plant leaf area. Moreover, the features, such as area, perimeter, major axis length, color and texture features, Convolutional Neural Network (CNN) feature, Local Gabor Binary Patterns (LGBP), Spider Local Image Features (SLIF) and Weber Local Descriptor (WLD) are extracted. Finally, cotton leaf disease is detected into healthy and non-healthy using EffNet_ShCNN, which is trained by STCWO. Here, STCWO is introduced by the incorporation of Siberian Tiger Optimization (STO) and

10.48047/jocaaa.2024.33.08.136

Carpet Weaver Optimization (CWO). Moreover, in the classification process, when the detected image is not healthy, the cotton leaf disease is classified into aphids, bacterial blight, healthy and targeted spot using STCWO_EffNet_ShCNN.

The key phase of this article is expressed as,

- **Proposed STCWO_EffNet_ShCNN for cotton leaf disease classification:** The novelty of this research is to present a hybrid optimization-enabled DL for cotton leaf disease classification named EffNet_ShCNN. The hyperparameters of EffNet_ShCNN are efficiently tuned by the novel algorithm named STCWO, where the STCWO is designed by integrating STO and CWO. Moreover, if the detected image is not healthy, the classification process is done utilizing STCWO_EffNet_ShCNN.

The following sections describe the layout of STCWO_EffNet_ShCNN framework: Section 2 explains the conventional models utilized in this research during the evaluation. Section 3 presents the STCWO_EffNet_ShCNN methodology with a brief explanation. Section 4 discusses the performance and comparative assessment based on existing approaches. Section 5 describes the conclusion of STCWO_EffNet_ShCNN with future work.

2. Motivation

In textile industries, cotton is widely used as a raw material. Nowadays, cotton faces significant issues with its healthy growth due to several diseases. These kinds of diseases minimize productivity, which causes financial loss for farmers due to crop loss. Manual observation of detecting the disease by farmers is time-consuming, and cost-effective as well as identification of cotton leaf disease at an early phase is a very complex task for the farmers. Therefore, the researchers are inspired to introduce a system for identifying and classifying the disease in cotton leaf by mitigating the issues of existing modules.

2.1 Literature Survey

X. Liang, [11] designed S-DenseNet for classifying cotton leaf spot disease. This approach effectively recovered useful information and prevented information loss. Nevertheless, this model was inherently handled with limited labeled data, which led to overfitting. M. Shao, *et al.* [12] developed Bilinear Coordinate Attention Enhancement Mechanism (BCAEM) in identifying cotton leaf diseases. Even though this method provided decision support for timely diagnosis, it did not consider lightweight network techniques to be more valid for agricultural production. S. Takkar, *et al.* [13] introduced Super-Resolution Convolutional Neural Network (SRCNN) in recognizing image-based plant leaf diseases. This model learned relevant features from raw images without feature engineering, making it easier and faster. Nevertheless, inaccurate labels lead to inaccurate training and poor performance. A. Magsi, *et al.* [14] established CNN for identifying the severity level of cotton plants. This module was efficient for local and global harvesters and also utilized to take time-based preventive measures for reducing loss percentage. However, it was unable to enhance the accuracy by raising the number of features and classification modules.

R. Nazeer, *et al.* [15] presented CNN for detecting the susceptibility scale level of cotton leaf curl disease. This approach supported sustainable agricultural practices all over the world. Nevertheless, it did not consider a broad range of ecological circumstances and a large database with several regions. R. Kumar, *et al.* [16] developed Random Forest and Decision Tree in detecting cotton crop disease. This module highlighted the importance of continuous enhancement by periodically determining the approaches and exploring the potential of improved models like DL. But it did not investigate alternative fusion models to combine predictions from diverse techniques to improve the robustness. Y. Shao, *et al.*

10.48047/jocaaa.2024.33.08.136

[17] designed CANnet to recognize cotton disease in natural environment. Although this model obtained maximum recognition rate, it did not design the features and characteristics of disease data and develop an effective network architecture. A. Shrotriya, *et al.* [18] established CNN+RNN for multimodal cotton plant disease detection. This system emphasized the potential of incorporating different data streams for providing a general interpretation of plant health, enabling reliable disease diagnosis. Nonetheless, it failed to design the module in real-time detection techniques to identify and treat diseased cotton plants in agricultural fields.

2.2 Challenges

The difficulties that exist in previous methods are enlisted beneath,

- In [11], the designed technique reduced irrelevant information in the image. However, it did not design a superior data generation technique and low-shot learning technique with uttermost generalization to enhance the robustness with fewer training parameters.
- An approach developed in [12] obtained less probability of misclassification for every type of disease and strong ability for extracting subtle features. Nonetheless, it only utilized most of the samples of medium to high-level disease images and a smaller number of images of early disease.
- The method introduced in [13] provided consistent results. But the technique trained in one environment was not generalized well due to variations in plant species, growth stages, lighting conditions, or background noise.
- Although the technique introduced in [14] only processed with single image of plucked leaves, it failed to perform with numerous images concurrently with other classification models.
- Detecting and classifying the diseases of cotton leaf utilizing several techniques, particularly DL and ML approaches attained better prominence due to the increasing impact of plant diseases on crop yield. However, the presence of various overlapping diseases on a single plant complicates the classification efforts. Moreover, ensuring timely and precise disease identification is important for efficient crop management, yet achieving this under diverse and dynamic field conditions remains a difficult task. Thus, a new model is proposed to mitigate these issues.

3. Proposed Siberian Tiger Carpet Weaver Optimization based EfficientNet-Fuzzy-Sheperd Convolutional Neural Network for cotton disease classification

Cotton diseases extremely impact the quality and yield of cotton. The particular disease affecting the cotton plant is identified by examining the disease spots on cotton leaves. Most viruses that harm the crops significantly also affect the cotton. The classification of leaf diseases suffers from some issues, like difficulty in evaluating the entire level of damage, precise diagnosing diseases with similar symptoms, and risk of misclassification. Thus, a module for cotton leaf disease classification is designed named STCWO_EffNet-ShCNN. From the dataset [19], a cotton leaf image is taken and subjected to pre-processing phase by utilizing Geometric Mean Filtering [20] to eliminate the noise. After that, plant area segmentation is carried out using ROSE [21]. In feature extraction process, features like LGBP [22], SLIF [23] and WLD [24], area, perimeter, major axis length [25], color and texture features [26], CNN [27], are extracted. Moreover, cotton leaf detection is done by STCWO_EffNet-ShCNN. Here, EffNet-ShCNN is the integration of EfficientNet [28], fuzzy concept [29] and ShCNN [30]. Here, the detected disease is categorized into healthy and non-healthy. Here, STCWO is the integration of STO [31] and CWO [32]. If the detected output is non-healthy, the cotton leaf disease is classified into aphids, bacterial blight, healthy and targeted spot by STCWO_EffNet-ShCNN in classification process. Figure 1 represents schematic diagram of cotton leaf disease classification using STCWO_EffNet-ShCNN.

10.48047/jocaaa.2024.33.08.136

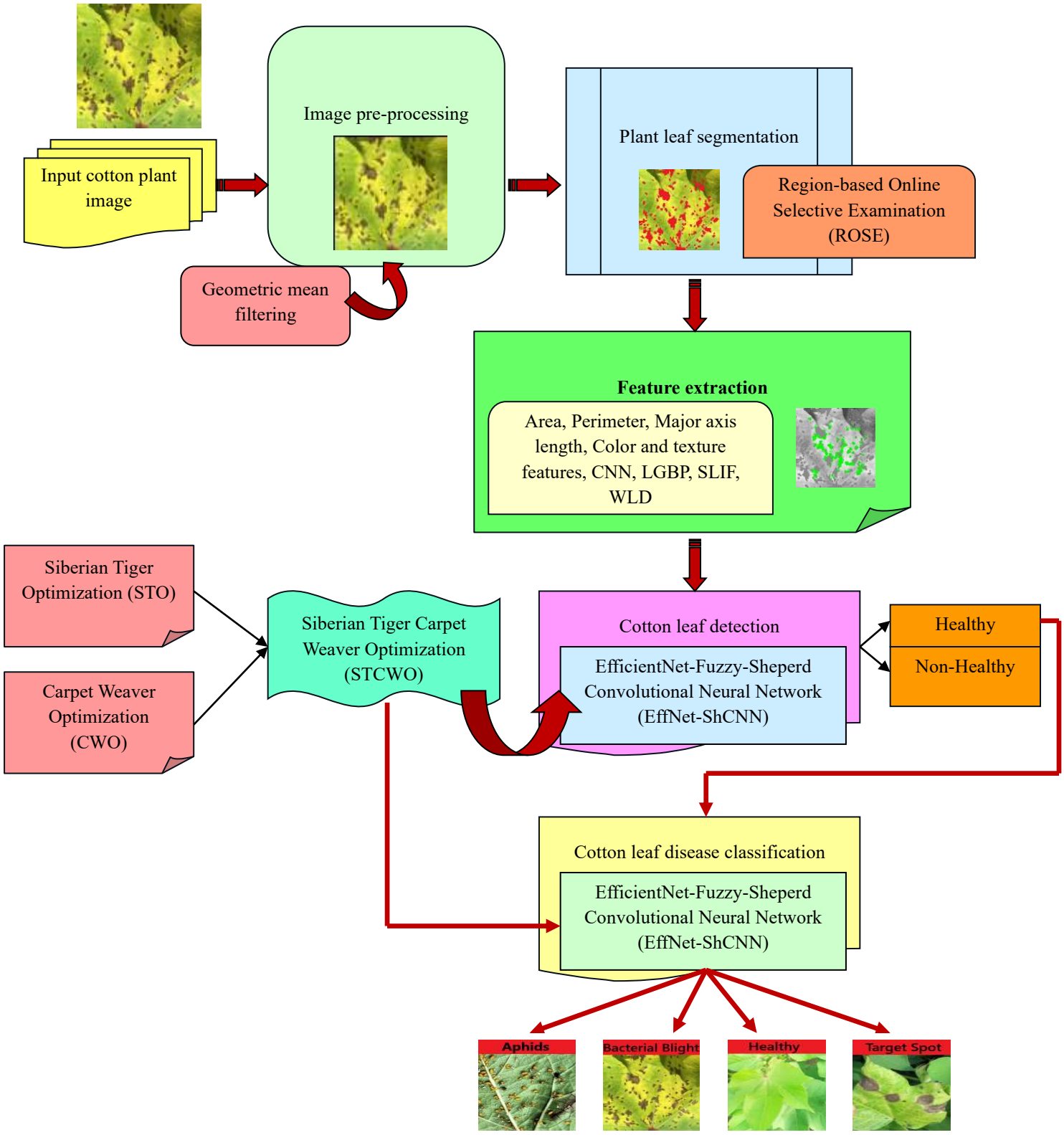

Figure 1. Schematic view of STCWO_EffNet-ShCNN for cotton leaf disease classification

10.48047/jocaaa.2024.33.08.136

3.1 Image Acquisition

A typical database Cotton Plant Disease [19] is symbolized as $'\mathrm{K}'$, which is composed of five Black and white with one directory. Here, $'\nu'$ number of images are present in $'\mathrm{K}'$, which is enumerated as,

$$\mathrm{K} = \left\{ \mathrm{K}_1, \mathrm{K}_2, ...\mathrm{K}_\mu, ...\mathrm{K}_\nu \right\} \tag{1}$$

Thereby, K_μ signifies input cotton leaf image, K_ν explicates overall images.

3.2 Pre-processing using Geometric mean filtering

It is processed to remove noise or unwanted variations in the pixel values, making it complex to identify the features. Here, the image K_μ is pre-processed by utilizing Geometric mean filtering.

3.2.1 Geometric Mean Filtering

It is utilized to find the mean of the sequence of numbers. Moreover, it obtains smoothing and loses less amount of image information when compared to the arithmetic mean filter. The computation of this filtering process [20] is determined as,

$$f\left(\varsigma,\zeta\right) = \left[\prod_{(c,d)\in \mathrm{E}_{\varsigma\zeta}} \Re\left(c,d\right) \right]^{\frac{1}{o\rho}} \tag{2}$$

Here, c,d defines abscissa and ordinate of pixels in a region determined by $\mathrm{E}_{\varsigma\zeta}$, $\Re\left(c,d\right)$ indicates pixel values at coordinates $\left(c,d\right)$ and $\mathrm{E}_{\varsigma\zeta}$ implies a set of coordinates in a rectangular sub-image window of size $o \times \rho$. The pre-processed image's pixel is $\frac{1}{o\rho}$ of the pixel product in the window. The dimension of this filter is enumerated as $o = \rho$. Hence, the filtered image is referred to as O_μ.

3.3 Plant leaf area segmentation using ROSE

It is a process of segmenting leaf area from filtered image O_μ for determining its size or analyzing its features, where this process is carried out by utilizing ROSE, since it allows for accurate segmentation from their background that makes simple to measure the region more precisely. Moreover, it also differentiates the leaves efficiently even in complex conditions.

3.3.1 ROSE

ROSE [21] is designed by utilizing Siamese structure that is composed of Region Prior Generation (RPG), Region Voting (RV) and Cross view Selective Examination (CSE). With the input image O_μ, a prior region U is generated using RPG and transform an image and prior region to a secondary view O_μ^{ℓ} and U^{ℓ}. After that, O_μ and O_μ^{ℓ} is subjected to segmentation phase for extracting deep features G and G^{ℓ} also $\hat{H}$ from main branch. Thereafter, region average pooling is used to acquire region-level features

10.48047/jocaaa.2024.33.08.136

$\mathrm{M}=\left\{\mathrm{M}_1,\mathrm{M}_2,....\mathrm{M}_\eta\right\}$ and $\mathrm{N}=\left\{\mathrm{N}_1,\mathrm{N}_2,....\mathrm{N}_\eta\right\}$. Here, η specifies number of regions. Moreover, region-level pseudo-label $b=\left\{b_1,b_2,....b_\eta\right\}$ and region-level prediction $\hat{b}=\left\{\hat{b}_1,\hat{b}_2,....\hat{b}_\eta\right\}$ are acquired using RV. This region-level information is employed in CSE for observing high-level corrected labels $b^*=\left\{b_1^*,b_2^*,....b_\eta^*\right\}$. Then, it is transformed into a pixel-level corrected label Z^*. At last, the corrected label Z^* is used as new supervision signal for training the model.

a) RPG

Here, the region priors are generated by using Segment Anything Model (SAM). Consider O_μ that automatically generates η masks $U\in\{0,1\}^{\eta\times\chi\times\varepsilon}$. RPG combines η masks to design unified map in bottom-up manner. Initially, η masks U are sorted using the region dimensions. After that, the overlap ratio for all maps is calculated. Consider a mask U_u as an instance, its overlap ratio with another mask U_v is determined by,

$$\Im\left(U_u,U_v\right)=\frac{\sum\left(U_u\otimes U_v\right)}{\sum U_u} \tag{3}$$

Here, $\otimes$ indicates Hadamard product. When the ratio is maximum than pre-determined threshold value, U_u is removed since it is more likely to be designed by U_v. This process is frequently performed till overall masks are validated.

b) RV

This phase extracts the region-level visual information with a winner-take-all voting system, which involves predictions and pseudo-labels. The plurality voting is designed for pseudo-labels Z for achieving region-level labels. Particularly, the category with maximum value of pixels is considered a region-level label, which is determined as,

$$b_f=\arg\max_{\kappa}\sum_{e}\mathrm{Z}_e\cdot\left\|\left(\square_e=f\right)\right. \tag{4}$$

Here, b_f symbolizes region-level pseudo-label for f^{th} region and e indexes spatial locations. $\left\|(\cdot)\right.$ returns 1 when an argument is true or else 0, $(\cdot)$ implies dot product. For predicting the model $\hat{\mathrm{Z}}\in\Im^{\chi\times\varepsilon\times\delta}$, its region-level prediction is same that is given as,

$$\hat{b}_f=\arg\max_{\kappa}\sum_{e}Hard\max_{\kappa}\left(\hat{\mathrm{Z}}_e\right)\cdot\left\|\left(\square_e=f\right)\right. \tag{5}$$

Here, $\hat{b}_f$ represents region-level predicted label for f^{th} region. Here, $Hard\max(\cdot)$ results in 1 for the category with maximum logit, else it results in 0.

c) CSE

10.48047/jocaaa.2024.33.08.136

This phase identified potential errors in annotations and corrected them using selective rules. Using region-level labels and predictions, new labels are attained through direct fusion method. Nonetheless, it was unable to analyze the feasibility of detections that results in a smaller number of corrected labels. Thus, the corrected process is performed as cross-view examination issue. This process is composed of cyclic exploration and selective correction.

i) Cyclic exploration: The features are determined and captured in several aspects using cycle consistency. It is significant is to design a suitable cycle pair. Here, a Siamese network is adopted that is composed of main and auxiliary branches. These two branches have parallel weights and architecture. The input for primary branch is $\mathrm{O}_{\mu} \in \Im^{\chi \times \varepsilon \times 3}$ and auxiliary branch is a transformed version of $\mathrm{O}_{\mu} = \phi\left(\mathrm{O}_{\mu}\right) \in \Im^{\chi^{\ell} \times \varepsilon^{\ell} \times 3}$. Here, $\phi(\cdot)$ indicates affine transformation function. Consequently, region prior $U^{\ell} = \phi(U)$ is converted by utilizing a similar affine transformation for matching spatial dimension of image. Then G is extracted by using network forward that is determined as,

$$\Psi_{f} = \frac{\sum_{e=1} G_{e} \cdot \left\| \left(\square_{e} = f \right) \right.}{\sum_{e=1} \left\| \left(\square_{e} = f \right) \right.} \tag{6}$$

Here, Ψ_{f} implies region-level features for f^{th} region and e enumerates spatial location indices. cross-view cyclic exploration is adopted and starts by determining cross-view affinity matrix that is enumerated as $\Phi \in \Im^{\eta \times \eta}$ that estimate the similarity between region features that is expressed as,

$$\Phi\left(e, f\right) = \frac{\omega_{e} \cdot \varpi_{f}}{\left\| \omega_{e} \right\| \cdot \left\| \varpi_{f} \right\|}, \ \forall e, f \tag{7}$$

For e^{th} region in main branch, the index of subsequent region in auxiliary branch is computed by,

$$f^{*} = \arg\max_{f} \Phi\left(e, f\right) \tag{8}$$

Here, $e \in \left[1, 2, ..., \eta\right]$ indicates region index. Thus, f^{*} region in auxiliary branch is considered as initial point for attaining e^{*th} index of similar region from main branch that is enumerated as,

$$e^{*} = \arg\max_{e} \Phi\left(e, f\right) \tag{9}$$

Here, e^{*} signifies Most Consistent Region (MCR) of e^{th} region.

ii) Selective correction: MCR is used to determine the correctness of label. When pseudo-label b_{e} is similar to MCR label for e^{th} region $b_{e^{*}} = b_{e}$, the pseudo-label of e^{th} region is assumed as correct label. When $b_{e^{*}} \neq b_{e}$ it is considered as incorrect, thus model prediction is used to correct the incorrect labels. When $\hat{b}_{e}$ given a constant response by cyclic exploration $\hat{b}_{e^{*}} = \hat{b}_{e}$, the label is corrected to $\hat{b}_{e}$. Otherwise,

10.48047/jocaaa.2024.33.08.136

this region was unable to find a constant area in pseudo-labels and predictions, thus it eliminates the present iteration of training process. Hence, the resultant region-level label b_e^* is corrected using,

$$b_e^* = \begin{cases} b_e, & if \quad b_{e^*} = b_e \\ \hat{b}_e, & else\, if \;\; \hat{b}_{e^*} = \hat{b}_e \\ 255, & otherwise \end{cases} \tag{10}$$

Even though, the corrected region-level labels have been identified, the images are losing their semantic contents through image transformations, which leads to unreliable MCR. Hence, the difference between forward and backward search and enumerate new cyclic score as $\Upsilon \in \Im^{\eta}$. It is determined using a product of forward and backward score as $\Phi\left(e, f^*\right)$ and $\Phi\left(f^*, e^*\right)$ that is determined as,

$$\Upsilon\left(e\right) = \Phi\left(e, f^*\right) \cdot \Phi\left(f^*, e^*\right) \tag{11}$$

When some objects provide high appearance variations in two types owing to image transformation, the inaccurate forward mostly generates minimal forward score that results in $\Upsilon\left(e\right)$. to minimize the training process, region confidences $\psi = \left\{\psi_1, \psi_2, ...\psi_{\eta}\right\} \in \Im^{\eta}$ are designed based on cyclic score and it represents feasibility of label correction. It is computed as,

$$\psi_e = \begin{cases} \Upsilon\left(e\right), & if \;\; \Upsilon\left(e\right) < \tau \\ 1, & otherwise \end{cases} \tag{12}$$

Here, τ implies a pre-determined threshold value.

d) Loss function

The region-level corrected labels $b^* = \left\{b_1^*, b_2^*, ..., b_{\eta}^*\right\}$ are transformed into pixel-level one-hot labels $Z^* \in \left\{0,1\right\}^{\chi \times \varepsilon \times \delta}$ on basis of combined region priors. A similar reverse function is performed on region confidence ψ for attaining confidence map $\psi \in \left\{0,1\right\}^{\chi \times \varepsilon}$. Therefore, pixel-level cross-entropy loss is determined with corrected labels Z_e^* and subsequent confidence ψ_e that is described as,

$$S = \frac{\sum_{e=1}^{\chi \times \varepsilon} \psi_e \cdot Z_e^* \log\left(\hat{b}_e\right)}{\sum_{e=1}^{\chi \times \varepsilon} \psi_e} \tag{13}$$

The segmented region of the plant leaf is symbolized as I_{μ}. Figure 2 demonstrates the general representation of ROSE.

10.48047/jocaaa.2024.33.08.136

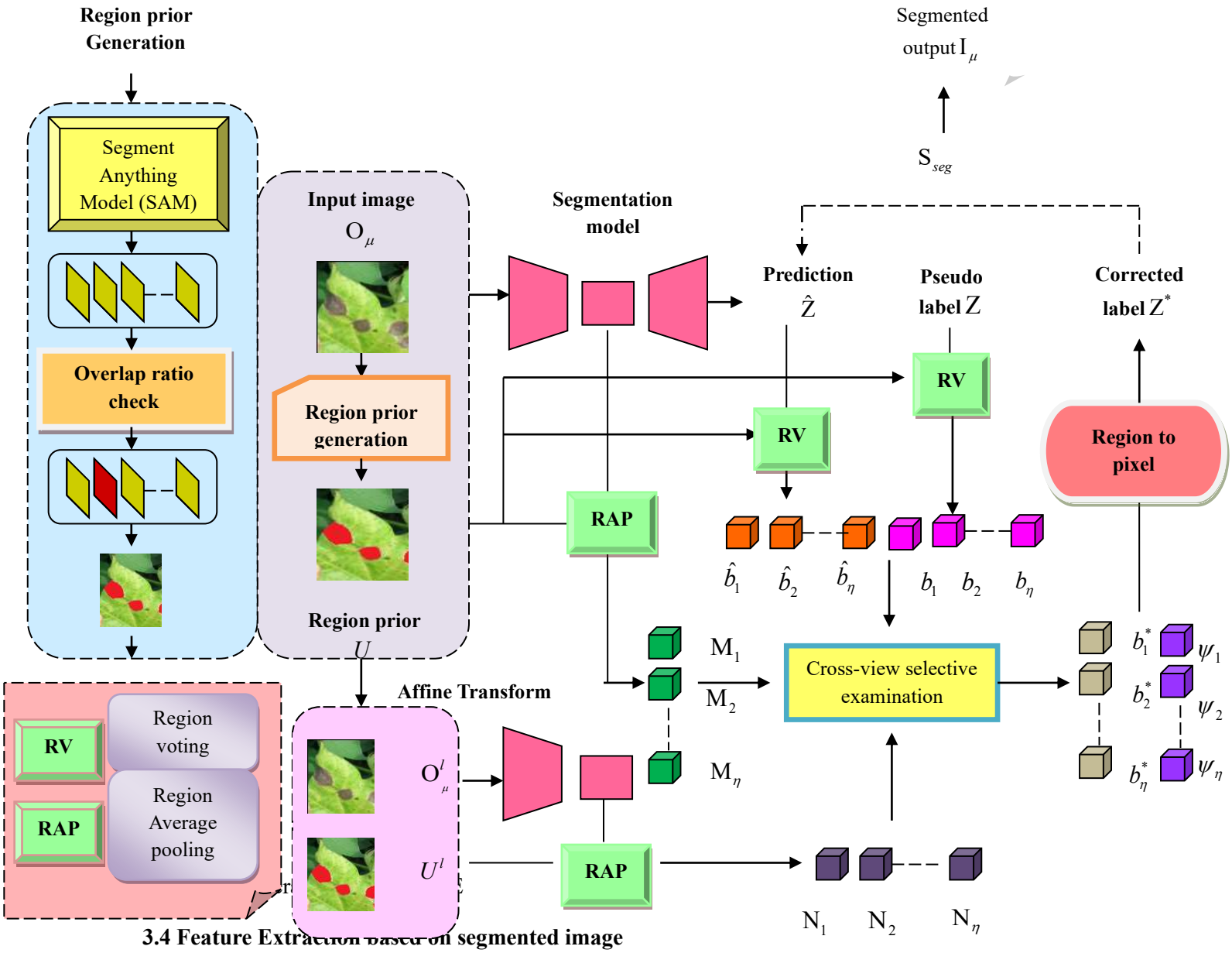

3.4 Feature Extraction based on segmented image

It is employed to minimize the actual data dimension. Moreover, it is also used to recognize and isolate the relevant features from cotton leaf images that can be utilized to differentiate between healthy and diseased plants. Here, the segmented image I_μ is considered for this process, where the features are listed below.

3.4.1 LGBP

Gabor features provide superior performance among overall features for image representation, which is utilized for diverse textures and local information [22]. 2D-Gabor filters are computed as,

10.48047/jocaaa.2024.33.08.136

$$\square_{\theta,\sigma}\left(\mathrm{I}_{\mu}\right)=\frac{\left\|\partial_{\theta,\sigma}\right\|}{\delta_{\hbar}^{2}}\exp\left[-\frac{\left\|\partial_{\theta,\sigma}\right\|^{2}\left\|\mathrm{I}_{\mu}\right\|}{2\delta_{\hbar}^{2}}\right]\left[\exp\left(k\partial_{\theta,\sigma}\cdot\mathrm{I}_{\mu}\right)-e\exp\left(\frac{\delta_{\hbar}^{2}}{2}\right)\right] \tag{14}$$

Here, θ,σ expresses Gabor kernel's position and size, $\delta_{\hbar}$ indicates Gaussian window size, $f_{\varpi,\sigma}$ enumerates wave vector and $\mathrm{B}_{1}^{\prime}$ depicts LGBP.

3.4.2 SLIF

It is considered for resolving the image matching issue [23] and it utilizes optimal allocation aspects of cross nodes with sphere web arrangement to perceptively extract visual images from all neighboring identified key points. It is computed as,

$$\square_{p,q}=\left(\frac{q\cdot\cos\left(\frac{2\pi p}{P}\right)}{Q},\frac{q\cdot\sin\left(\frac{2\pi p}{P}\right)}{Q}\right) \tag{15}$$

Here, primary and secondary requirements are similar to parallel and perpendicular coordinates of known nodes (o,p), as well as P and Q refer to radial and spiral fibers, $\square_{p,q}$ indicating position of all nodes subsequent to the initialization of 2D plane of coordinates. Here, $\mathrm{B}_{2}^{\prime}$ depicts SLIF.

3.4.3 WLD

WLD is an effective local texture descriptor for digital images designed on basis of Weber's Law [24].

a) Differential Excitation

The micro-variation in the configuration is computed through the estimation of intensity differentiation between neighboring pixels that is expressed as,

$$\varphi D=\sum_{L_l=0}^{N_n-1}\varphi D\left(Hh_{L_l}\right)=\sum_{L_l=0}^{N_n-1}D\left(Hh_{L_l}\right)-D\left(Hh_{E_e}\right) \tag{16}$$

Here, L_l^{th} neighbors of Hh_{E_e} are specified as $Hh_{L_l}\left(L_l=0,1,.....N_n-1\right)$ and N_n depict overall neighboring regions, $D\left(Hh_{L_l}\right)$ and $D\left(Hh_{E_e}\right)$ enumerate the potential of neighboring and current pixels.

b) Orientation

It selects directional elements of pixels and it is enumerated as,

$$\Theta\left(Hh_{E_e}\right)=\arctan\left(\frac{Z_z D_{V_v}}{Z_z D_{U_u}}\right), \tag{17}$$

10.48047/jocaaa.2024.33.08.136

Here, $Z_z D_{V_v} = D\left(Hh_7\right) - D\left(Hh_3\right)$ and $Z_z D_{U_u} = D\left(Hh_5\right) - D\left(Hh_1\right)$ is calculated from two filters. Thus, B_3' depicts WLD.

3.4.4 Area

It represents the overall pixels in the shape of an infected region [25]. It also determines the area of the infected region, where it differentiates from Blast and Brown spot diseased segmented images. It is expressed as h_1.

3.4.5 Perimeter

It is a substantial entity of an object. Here, contour-based features neglect the interior of shape based on identifying the perimeter or object's boundary points [25]. Thus, perimeter h_3 is indicated as,

$$\mathbf{Z} = m\left(l\right) + n\left(l\right) dl \tag{18}$$

3.4.6 Major Axis Length

It is determined using the possible combinations of perimeter pixels to identify the longest line [25], which is expressed as,

$$h_3 = \sqrt{\left(m_2 - m_1\right)^2 + \left(n_2 - n_1\right)^2} \tag{19}$$

Here, $\left(m_1, n_1\right)$ and $\left(m_2, n_2\right)$ indicates coordinates of two endpoints of major axis and h_3 enumerates major axis length.

Features like area, perimeter, and major axis length are applied to LGBP, SLIF and WLD. Hence, feature vector obtained from LGBP, SLIF and WLD is expressed as,

$$\mathrm{B}_1 = \left\{h_1^1, h_2^1, h_3^1\right\} \tag{20}$$

$$\mathrm{B}_2 = \left\{h_1^2, h_2^2, h_3^2\right\} \tag{21}$$

$$\mathrm{B}_3 = \left\{h_1^3, h_2^3, h_3^3\right\} \tag{22}$$

3.4.7 Color features

First, R, G and B components are extracted for affected region as well as mean value and standard deviation are determined. Then, extract H, S and V as well as evaluate median value from HSV technique. Lastly, extract L, A and B and determine median value from LAB color technique. The median and standard deviation [26] are determined using,

$$\mathrm{k}_j = \frac{1}{h} \sum_{i=1}^{h} \Omega_{ji} \tag{23}$$

10.48047/jocaaa.2024.33.08.136

$$\mathrm{A}_j = \sqrt{\frac{1}{h}\sum_{i=1}^{h}\left(\Omega_{ji} - \mathrm{k}_j\right)^2} \tag{24}$$

Here, k_j implies mean, A_j explicates standard deviation, Ω_{ji} indicates pixel values, h enumerates overall pixels. Thus, B_4 indicates color features.

3.4.8 Texture features

GLCM feature attains texture image through the spatial relationship among pair of gray value intensity pixels. Here, homogeneity, correlation, energy and contrast are utilized for extracted GLCM features [26]. The expressions of GLCM are determined as,

$$Hom_j = \sum_{i=0}^{h}\frac{\Omega_{ji}}{1+\left(j-i\right)^2} \tag{25}$$

$$corr_j = \sum_{i=0}^{h}\Omega_{ji}\frac{\left(j-\mathrm{k}\right)\left(i-\mathrm{k}\right)}{\mathrm{A}_j} \tag{26}$$

$$cont_j = \sum_{i=0}^{h}\Omega_{ji}\left(j-i\right)^2 \tag{27}$$

$$Ener_j = \sum_{i=0}^{h}\left(\Omega_{ji}\right)^2 \tag{28}$$

Here, $Ener_j$ enumerates energy, $cont_j$ indicates contrast, $corr_j$ explicates correlation, Hom_j refers to homogeneity. Thus, B_5 defines texture features.

3.4.9 CNN feature

CNN module [27] is composed of convolutional layers, pooling layers and fully-connected layers. By stacking these three layers, CNN has been designed. The CNN is obtained from CNN layers. It is indicated as B_6.

Therefore, the feature vector B_μ is given as,

$$\mathrm{B}_\mu = \left\{\mathrm{B}_1, \mathrm{B}_2, ..., \mathrm{B}_6\right\} \tag{29}$$

3.5 Cotton leaf disease detection using STCWO-EffNet_ShCNN

Cotton is the most profitable crop in the world. Every year crop production suffers due to various diseases. Computerized techniques are utilized for detecting the disease at an early stage, which may minimize the loss in cotton production. Even though various techniques have been designed for cotton disease detection, some issues occur due to low-quality images and different backgrounds. Hence, STCWO-EffNet_ShCNN is proposed to solve the issues in cotton leaf disease detection. Here,

10.48047/jocaaa.2024.33.08.136

EffNet_ShCNN is used to detect the leaf disease of cotton, whereas STCWO is utilized for tuning the hyperparameters of EffNet_ShCNN module. In this process, B_μ is used for identifying the disease of cotton leaves.

3.5.1 Structure of EffNet_ShCNN module

The EffNet_ShCNN module is composed of EfficientNet, EffNet_ShCNN layer and ShCNN structures. First, K_μ is given as an input for EfficientNet and its outcome is symbolized as $A_{\mu 1}$. After that, $A_{\mu 1}$ and B_μ is forwarded to EffNet_ShCNN layer. Here, the fusion and fuzzy concept is performed, where the fusion is used to combine the two approaches and fuzzy is used to modify the layers of networks. The resultant of EffNet_ShCNN layer is $A_{\mu 2}$, which is subjected to ShCNN with input K_μ. Hence, the detected output is specified as $A_{\mu 3}$. Figure 3 illustrates general view of EffNet_ShCNN module.

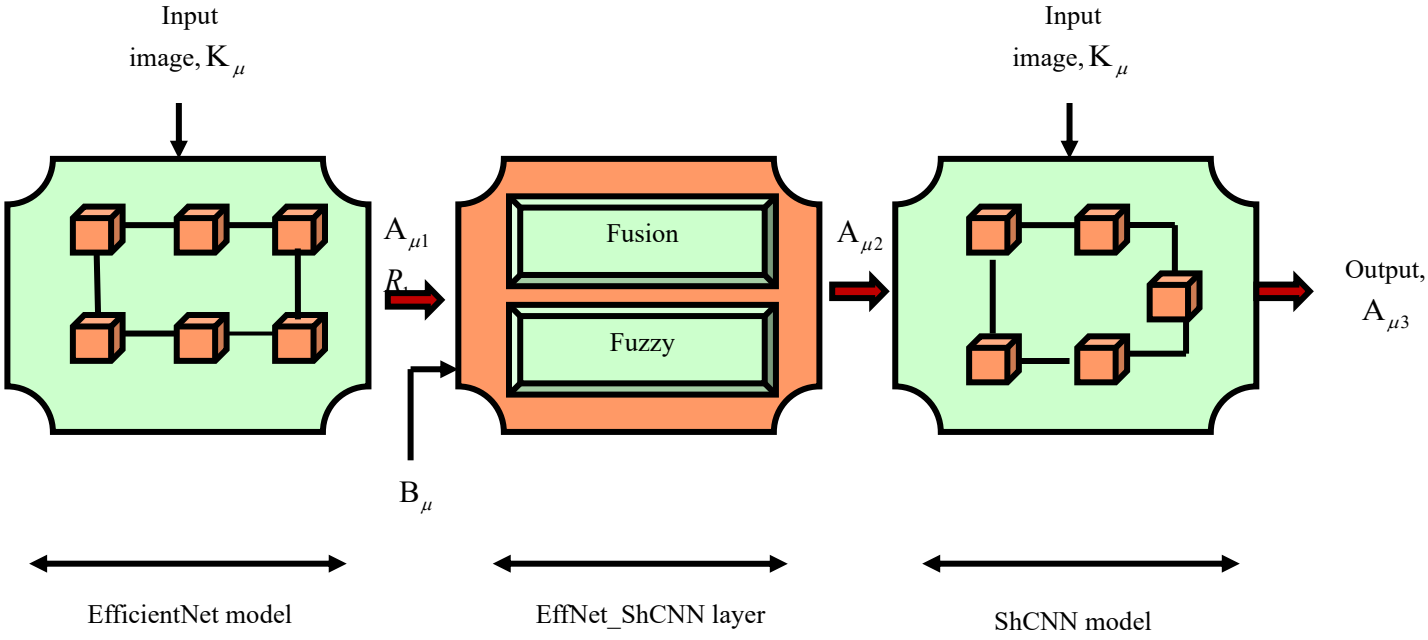

Figure 3. General view of EffNet_ShCNN module

a) EfficientNet

EfficientNet [28] is employed as the efficient mixing coefficient. Apart from preceding techniques of scaling characteristics of networks, like width, depth, and resolution, it uniformly estimates all dimensions with consistent scaling factors, where its particular dimension improves the performance of representation and weighing all sizes based on accessible resources efficiently improves overall efficiency.

Considering the input vector as r_s, characteristic map as t_w, attention vector as $k_w \in [0,1]^{\psi}$, attention glimpse as $\wp_w$ and attention network as $E_\tau(r_s)$. The attention mechanism is usually expressed as,

10.48047/jocaaa.2024.33.08.136

$$k_w = E_\tau\left(r_s\right) \tag{30}$$

The resultant of Efficient-B3_Attn2 $\mathrm{A}_{\mu 1}$ is computed as,

$$\mathrm{A}_{\mu 1}\left(\wp_w\right) = k_w \otimes t_w \tag{31}$$

Here, $\otimes$ indicates element-wise multiplication. The attention model obtains the values $k_w \in [0,1]^{\psi}$ between 0 and 1.

b) Efficient_ShCNN layer

Fuzzy rule-based techniques [29] are majorly used to control problems. Meanwhile, classification problems are entirely different, thus, the fuzzy control methods are not eligible to apply on fuzzy rule-based classification techniques. In this layer, B_{μ} and $\mathrm{A}_{\mu 1}$ are given as the input and thus provided the outcome as,

$$\mathrm{A}_{\mu 2} = \lambda_{XY} \approx \max\left\{\lambda_{X_1}, \lambda_{X_2}, ..., \lambda_{X_N}\right\} \tag{32}$$

Here, $\mathrm{A}_{\mu 2}$ represents Efficient_ShCNN layer output.

c) ShCNN model

ShCNN [30] weighs known pixels are different under their spatial distances to the processed pixel. Particularly, Shepard model is rewritten in convolution as,

$$\mathrm{A}_{\mu 3} = \begin{cases} \left(W * \mathrm{A}_{\mu 2}\right)_y \Big/ \left(W * V\right)_y & if\ V_y = 0 \\ \mathrm{A}_{\mu 2_y} & if\ V_y = 1 \end{cases} \tag{33}$$

Here, y enumerates image maps, V signifies binary function, $V_y = 0$ expresses pixel values are unidentified, $*$ symbolizes conv process, W signifies kernel function whose weights are reciprocally based on distance among pixel with $V_y = 1$ and pixel to function. Thus, ShCNN output is indicated as $\mathrm{A}_{\mu 3}$.

3.5.2 Algorithm of STCWO

STO [31] is a metaheuristic algorithm that is designed by the natural behavior of Siberian tigers which means their strategy of hunting prey and their technique to fighting brown bears are intelligent processes. The Siberian tigers select their prey during hunting and then attack it. At last, the prey will be hunted in chasing process. Due to the conflicts over prey, The Siberian tigers fight with black and brown bears and protect themselves. CWO [32] is inspired by the skill of carpet weaving process. Thus, integrating STO and CWO, a novel STCWO is designed, which efficiently detects cotton leaf diseases with higher accuracy by minimizing errors.

a) Solution Encoding

10.48047/jocaaa.2024.33.08.136

It is considered to represent potential solutions to an optimization problem in a given search space (λ) that is determined by,

$$\lambda = [1 \times \square] \tag{34}$$

Here, $\square$ is a learning factor of EffNet_ShCNN.

b) Fitness value

The location of all candidates in (λ) determines the values of problem. Thus, corresponding to all candidates, it is evaluated as,

$$\mathrm{F} = \frac{1}{\nu}\sum_{\mu=1}^{\nu}\left[\zeta_{\mu} - \mathrm{A}_{\mu 3}\right]^2 \tag{35}$$

Here, ζ_{ν} and A_{ν} depicts targeted and detected output.

c) Algorithmic steps

The steps performed for the new algorithm STCWO are elaborated as,

Step 1: Initialization

The population of STO seeks superior solutions by shifting their positions. It is also known as candidate solution to problem, where its location indicates problem's variables. It is calculated using,

$$B = \left\{B_1, B_2, ...B_{\hbar,\lambda}, ...B_{C,a}\right\} \tag{36}$$

Here, B implies location of population members, $B_{\hbar}$ enumerates $\hbar^{th}$ candidate solutions and C defines overall candidate solutions. The first position of candidate solution is arbitrarily computed as,

$$B_{\hbar,\lambda} = LB_{\lambda} + \vartheta_{\hbar,\lambda} \cdot \left(UB_{\lambda} - LB_{\lambda}\right), \quad \hbar = 1, 2, ..., C; \lambda = 1, 2, ..., a \tag{37}$$

Here, $B_{\hbar,\lambda}$ indicates λ^{th} dimension of $B_{\hbar}$ in problem variable, a enumerates overall problem values, $\vartheta_{\hbar,\lambda}$ represents arbitrary values ranging $[0,1]$, $UB_{\lambda}, LB_{\lambda}$ indicates upper and lower bounds of λ^{th} problem variable.

Step 2: Determine fitness

The value of objective function is analyzed based on each Siberian tiger, which is mentioned in Eq. (35).

Step 3: Prey Hunting

Through the simulation of prey hunting process, the members are determined. Once prey is chosen, Siberian tiger attacks and kills them in chasing process. Here, two stages are followed and simulated. In

10.48047/jocaaa.2024.33.08.136

the first stage, the member's position is determined through the selection and prey attack. It creates sudden and wide variations in member's positions. Thus, it improves the potential of global search and exploration of algorithm. The prey positions for all members are chosen from other members with superior fitness values. The set of positions is computed as,

$$AT_{\hbar} = \left\{ B_o \,\middle|\, o \in \{1,2,.....,C\} \wedge \mathrm{F}_o < \mathrm{F}_{\hbar} \right\} \cup \left\{ B_{best} \right\} \tag{38}$$

Here, B_{best} enumerates candidate solutions. Then, a particular member $M_{\hbar}$ from this set $AT_{\hbar}$, which is arbitrarily chosen as attacked target by $\hbar^{th}$ member and its new location is determined through attack simulation on prey by,

$$B_{\hbar,\lambda}^{ph_1 st_1} = B_{\hbar,\lambda} + \vartheta_{\hbar,\lambda} \cdot \left(M_{\hbar,\lambda} - S_{\hbar,\lambda} \cdot B_{\hbar,\lambda} \right), \quad \hbar = 1,2,....,C; \lambda = 1,2,.....,a \tag{39}$$

Thereby, $B_{\hbar,\lambda}^{ph_1 st_1}$ enumerates new position of $\hbar^{th}$ member of first stage of first phase $M_{\hbar,\lambda}$ indicates λ^{th} dimension of $M_{\hbar}$, $S_{\hbar,\lambda}$ specifies random values between $[1,2]$.

Let us consider,

$$B_{\hbar,\lambda}^{ph_1 st_1} = B_{\hbar,\lambda}(\delta + 1) \tag{40}$$

$$B_{\hbar,\lambda} = B_{\hbar,\lambda}(\delta) \tag{41}$$

$$M_{\hbar,\lambda} = M_{\hbar,\lambda}(\delta) \tag{42}$$

$$S_{\hbar,\lambda} = S_{\hbar,\lambda}(\delta) \tag{43}$$

Substituting Eq. (40), (41), (42), (43) in Eq. (39), then it is recomputed as,

$$B_{\hbar,\lambda}(\delta + 1) = B_{\hbar,\lambda}(\delta) + \vartheta_{\hbar,\lambda} \cdot \left(M_{\hbar,\lambda}(\delta) - S_{\hbar,\lambda}(\delta) \cdot B_{\hbar,\lambda}(\delta) \right) \tag{44}$$

$$B_{\hbar,\lambda}(\delta + 1) = B_{\hbar,\lambda}(\delta)\left[1 - S_{\hbar,\lambda}(\delta) \cdot \vartheta_{\hbar,\lambda} \right] + \vartheta_{\hbar,\lambda} \cdot M_{\hbar,\lambda}(\delta) \tag{45}$$

The update expression from CWO is combined since CWO has utmost efficiency in real-time applications that are expressed as,

$$\mathrm{X}_{\hbar\lambda}^{\mathrm{P}} = \mathrm{X}_{\hbar\lambda} + (1 - 2\upsilon)\left(\mathrm{X}_{\mathrm{P},\lambda} - A \cdot \mathrm{X}_{\hbar\lambda} \right) \tag{46}$$

Here, $\mathrm{X}_{\mathrm{P},\lambda}$ defines λ^{th} dimension, $\mathrm{X}_{\hbar\lambda}^{\mathrm{P}}$ implies λ^{th} dimension of first phase, υ indicates arbitrary value within $[0,1]$, A refers to arbitrarily selected value between $[1,2]$.

Let us consider, $\mathrm{X}_{\hbar\lambda}^{\mathrm{P}} = B_{\hbar,\lambda}(\delta + 1)$, $\mathrm{X}_{\hbar\lambda} = B_{\hbar,\lambda}(\delta)$, $\mathrm{X}_{\mathrm{P},\lambda} = \mathrm{X}_{\mathrm{P},\lambda}(\delta)$ and substitute them in Eq. (46),

10.48047/jocaaa.2024.33.08.136

$$B_{\hbar,\lambda}(\delta+1)=B_{\hbar,\lambda}(\delta)+(1-2\upsilon)\left(\mathrm{X}_{\mathrm{P},\lambda}(\delta)-A\cdot B_{\hbar,\lambda}(\delta)\right) \tag{47}$$

$$B_{\hbar,\lambda}(\delta+1)=B_{\hbar,\lambda}(\delta)\left[1-A(1-2\upsilon)\right]+(1-2\upsilon)\mathrm{X}_{\mathrm{P},\lambda}(\delta) \tag{48}$$

$$B_{\hbar,\lambda}(\delta)=\frac{B_{\hbar,\lambda}(\delta+1)-(1-2\upsilon)\left(\mathrm{X}_{\mathrm{P},\lambda}(\delta)\right)}{\left[1-A(1-2\upsilon)\right]} \tag{49}$$

Substitute Eq. (49) in Eq. (45), then

$$B_{\hbar,\lambda}(\delta+1)=\left[\frac{B_{\hbar,\lambda}(\delta+1)-(1-2\upsilon)\left(\mathrm{X}_{\mathrm{P},\lambda}(\delta)\right)}{\left[1-A(1-2\upsilon)\right]}\right]\left[1-S_{\hbar,\lambda}(\delta)\cdot\vartheta_{\hbar,\lambda}\right]+\vartheta_{\hbar,\lambda}\cdot M_{\hbar,\lambda}(\delta) \tag{50}$$

$$B_{\hbar,\lambda}(\delta+1)-\frac{B_{\hbar,\lambda}(\delta+1)}{\left[1-A(1-2\upsilon)\right]}\left[1-S_{\hbar,\lambda}(\delta)\cdot\vartheta_{\hbar,\lambda}\right]=\left[\frac{\begin{array}{r}(2\upsilon-1)\left(\mathrm{X}_{\mathrm{P},\lambda}(\delta)\right)\left[1-S_{\hbar,\lambda}(\delta)\cdot\vartheta_{\hbar,\lambda}\right]\\+\vartheta_{\hbar,\lambda}\cdot M_{\hbar,\lambda}(\delta)\end{array}}{\left[1-A(1-2\upsilon)\right]}\right] \tag{51}$$

$$\frac{B_{\hbar,\lambda}(\delta+1)\left[1-A(1-2\upsilon)-1+S_{\hbar,\lambda}(\delta)\cdot\vartheta_{\hbar,\lambda}\right]}{\left[1-A(1-2\upsilon)\right]}=\left[\frac{\begin{array}{r}(2\upsilon-1)\left(\mathrm{X}_{\mathrm{P},\lambda}(\delta)\right)\left[1-S_{\hbar,\lambda}(\delta)\cdot\vartheta_{\hbar,\lambda}\right]\\+\vartheta_{\hbar,\lambda}\cdot M_{\hbar,\lambda}(\delta)\end{array}}{\left[1-A(1-2\upsilon)\right]}\right] \tag{52}$$

$$B_{\hbar,\lambda}(\delta+1)=\left[\frac{(2\upsilon-1)\left(\mathrm{X}_{\mathrm{P},\lambda}(\delta)\right)\left[1-S_{\hbar,\lambda}(\delta)\cdot\vartheta_{\hbar,\lambda}++\vartheta_{\hbar,\lambda}\cdot M_{\hbar,\lambda}(\delta)\right]\left[1-A(1-2\upsilon)\right]}{\left[S_{\hbar,\lambda}(\delta)\cdot\vartheta_{\hbar,\lambda}-A(1-2\upsilon)\right]}\right] \tag{53}$$

The newly determined position is adequate when it enhances the fitness value by updating STO members, which is expressed as,

$$B_{\hbar}=\begin{cases}B_{\hbar}^{ph_1 st_1}, & \mathrm{F}_{\hbar}^{ph_1 st_1}<\mathrm{F}_{\hbar}\\ B_{\hbar}, & else\end{cases} \tag{54}$$

Here, $\mathrm{F}_{\hbar}^{ph_1 st_1}$ indicates fitness value of $\hbar^{th}$ member $B_{\hbar}^{ph_1 st_1}$.

In second stage, the population member's position is determined through chasing process. The candidate alters its position in a region where it attacks the prey. It enhances the module's ability in local search as well as exploitation for reaching superior solutions. The new position for candidate solution near the attack site is determined for simulating the chasing process by utilizing,

10.48047/jocaaa.2024.33.08.136

$$B_{\hbar}^{ph_1 st_2} = B_{\hbar,\lambda} + \frac{\vartheta_{\hbar,\lambda}\left(UB_{\lambda} - LB_{\lambda}\right)}{g}, \quad \hbar = 1,2,....,C; g = 1,2,.....,\mathrm{T} \tag{55}$$

$$B_{\hbar} = \begin{cases} B_{\hbar}^{ph_1 st_2}, & \mathrm{F}_{\hbar}^{ph_1 st_2} < \mathrm{F}_{\hbar} \\ B_{\hbar}, & else \end{cases} \tag{56}$$

Here, $B_{\hbar}^{ph_1 st_2}$ implies new position of second stage, $\mathrm{F}_{\hbar}^{ph_1 st_2}$ is the fitness of second stage, and g implies iterations.

Step 4: Fighting with Bear

Observations of natural aspect of the candidates show that they are often fighting with black and brown bears over prey and to protect their lives. Hence, STO members are determined in second phase on basis of simulating the technique of candidate solutions by fighting the bears. They have two fighting strategies namely, attack and conflict. For modeling the attack of $\hbar^{th}$ tiger on bear, other population members are considered as set of bears in first stage. From this, the position of attacked bear is arbitrarily chosen that is specified as o . Thus, this algorithm has increased the global search of model and exploration capability due to the sudden variations in the STO member's position. As a result, a new position is determined for $\hbar^{th}$ STO members using,

$$B_{\hbar}^{ph_2 st_1} = \begin{cases} B_{\hbar,\lambda} + \vartheta_{\hbar,\lambda} \cdot \left(B_{o,\lambda} - S_{\hbar,\lambda} \cdot B_{\hbar,\lambda}\right), & \mathrm{F}_o < \mathrm{F}_{\hbar} \\ B_{\hbar,\lambda} + \vartheta_{\hbar,\lambda} \cdot \left(B_{\hbar,\lambda} - S_{\hbar,\lambda} \cdot B_{o,\lambda}\right), & else \end{cases} \tag{57}$$

Here, $B_{o,\lambda}$ indicates λ^{th} dimension of bear location, o represents randomly selected from $\{1,2,.....,\hbar-1,\hbar+1,.....,C\}$, $B_{\hbar}^{ph_2 st_1}$ enumerates new positions based on first stage of second phase.

When objective value is increased, this newly determined position replaces the former location of subsequent value. It is expressed as,

$$B_{\hbar} = \begin{cases} B_{\hbar}^{ph_2 st_1}, & \mathrm{F}_{\hbar}^{ph_2 st_1} < \mathrm{F}_{\hbar} \\ B_{\hbar}, & else \end{cases} \tag{58}$$

Here, F_o indicates fitness value of bear. In the second stage, the population members' position is computed through the simulation of conflicts during fight. It causes small variations in the position, which leads to enhancing local search and exploitation ability. Hence, arbitrary location near the fight location is determined by,

$$B_{\hbar}^{ph_2 st_2} = B_{\hbar,\lambda} + \frac{\vartheta_{\hbar,\lambda}}{g}\left(UB_{\lambda} - LB_{\lambda}\right), \quad \hbar = 1,2,....,C; \lambda = 1,2,.....,a; g = 1,2,.....,\mathrm{T} \tag{59}$$

10.48047/jocaaa.2024.33.08.136

Here, $B_{\hbar}^{ph_2\,st_2}$ enumerates new position of candidate solution based on second phase and stage. This new location is adequate for update process when it increases the fitness value using,

$$B_{\hbar}=\begin{cases}B_{\hbar}^{ph_2\,st_2}, & \mathrm{F}_{\hbar}^{ph_2\,st_2}<\mathrm{F}_{\hbar}\\ B_{\hbar}, & else\end{cases} \tag{60}$$

Here, $\mathrm{F}_{\hbar}^{ph_2\,st_2}$ indicates fitness value $B_{\hbar}^{ph_2\,st_2}$.

Step 5: Re-evaluate fitness

This determination is frequently performed to minimize the error in a solution for attaining optimal solution using Eq. (35).

Step 6: Termination

The above steps are iteratively carried out till it acquires a fine solution. Algorithm 1 shows the Pseudocode of STCWO.

Algorithm 1. Pseudocode of STCWO

SL. No	Pseudocode of STCWO
1	**Input:** Population size C , Fitness F , iteration g
2	**Output:** $B_{\hbar,\lambda}\left(\delta+1\right)$
3	**Begin**
4	Initialize the population by Eq. (36)
5	Determine fitness by Eq. (35)
6	For $g=1\ to\ \mathrm{T}$
7	For $\hbar=1\ to\ C$
8	**Prey hunting**
9	Determine prey set for $\hbar^{th}$ STO members by Eq. (38)
10	Estimate new position of $\hbar^{th}$ STO member of first stage by Eq. (39)
11	Update new solution by Eq. (53)
12	Evaluate $\hbar^{th}$ STO member by Eq. (54)
13	Estimate new position of $\hbar^{th}$ member of second stage by Eq. (55)
14	Evaluate $\hbar^{th}$ STO member by Eq. (56)
15	**Fighting with bear**
16	Choose a member as bear location B_o arbitrarily
17	Determine new position of $\hbar^{th}$ member of first stage by Eq. (57)
18	Evaluate $\hbar^{th}$ STO member by Eq. (58)
19	Compute new position of $\hbar^{th}$ member of first stage by Eq. (59)
20	Evaluate $\hbar^{th}$ STO member by Eq. (60)
21	end
22	Save superior candidate solution
23	end

10.48047/jocaaa.2024.33.08.136

24	**Return**
25	**Terminate**

3.6 Cotton leaf disease classification using STCWO-EffNet_ShCNN

In India, many crops have been cultivated by the farmers, but cotton is the most highly productive crop. Even though the production of cotton is high, crop loss is the prime issue due to leaf disease. Thus, early detection and appropriate management are significant in reducing the impact of these diseases on cotton yield. Moreover, disease classification is significant to accurately identify and diagnose leaf diseases early that enhances crop yield, enables timely treatment, and reduces economic losses. Therefore, EffNet_ShCNN is designed for classifying cotton leaf diseases. Here, EffNet_ShCNN is tuned by utilizing STCWO algorithm. The structure and algorithm of STCWO-EffNet_ShCNN are already explained in sections 3.5.1 and 3.5.2. Thus, the classified output is signified as H_{μ}. The classified diseases are Aphids, Bacterial blight, healthy and Target spot.

4. Results and Discussions

This section enumerates STCWO-EffNet_ShCNN framework with the existing modules and database description.

4.1 Experimental setup

The STCWO-EffNet_ShCNN is implemented in PYTHON tool to achieve better performance.

4.2 Dataset Description

Cotton plant disease database [19] is majorly composed of five diseases in cotton plants namely, Aphids, Army worms, Bacterial Blight. Powdery Mildew and Target Spot. Moreover, it includes healthy leaf database to compare with infected plants. Furthermore, it comprises 26.1k files, which are in jpg format.

4.3 Experimental outcomes

Figure 4 illustrates image results of STCWO-EffNet_ShCNN. Figure 4 illustrates Aphids and Bacterial blight diseases. Figure 4 a) represents input image-1, Figure 4 b) represents input image-2, Figure 4 c) specifies filtered image-1, Figure 4 describes d) filtered image-2, Figure 4 shows e) segmented image-1, Figure 4 f) elucidates segmented image-2, Figure 4 g) explicates LGBP-1, Figure 4 h) demonstrates LGBP-2, Figure 4 i) depicts SLIF-1, Figure 4 j) illustrates SLIF-2, Figure 4 k) enumerates WLD-1, Figure 4 l) expresses WLD-2, Figure 4 m) enumerates Aphids disease image, and Figure 4 n) elucidates Bacterial blight disease image.

(a)

(b)

10.48047/jocaaa.2024.33.08.136

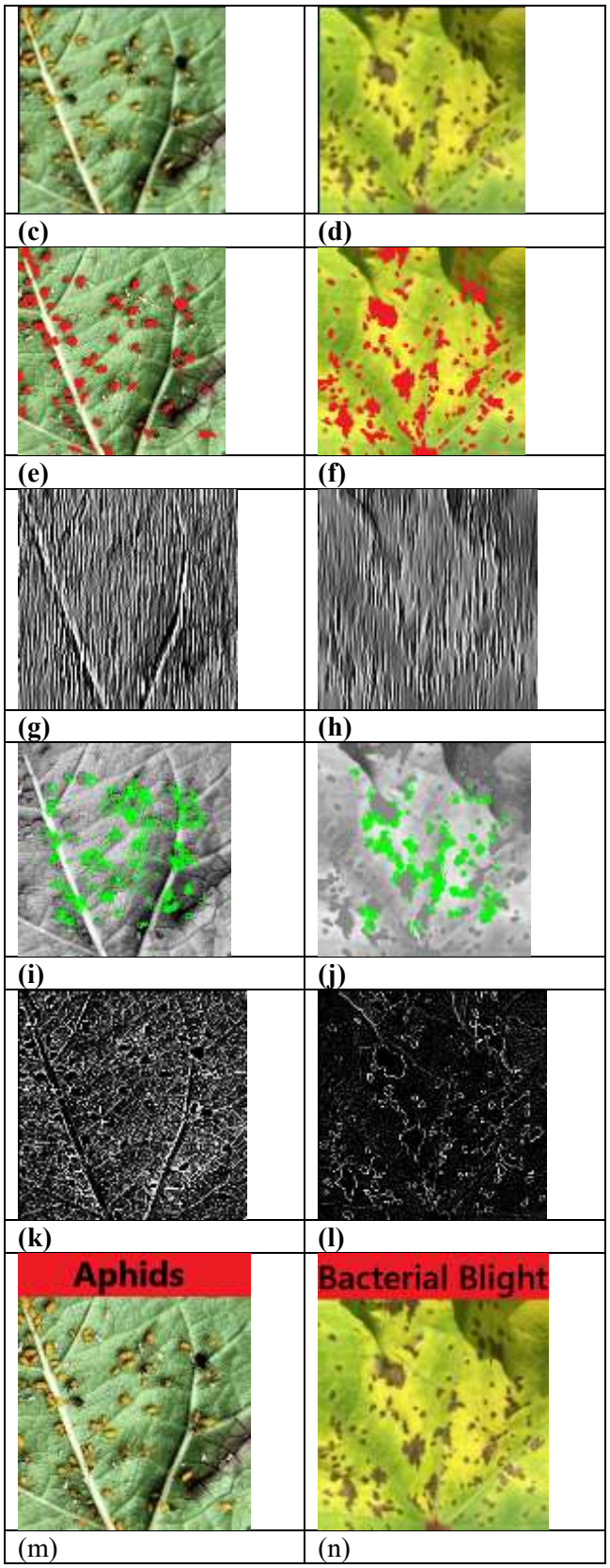

10.48047/jocaaa.2024.33.08.136

Figure 4. Image results of Aphids and Bacterial blight, a) input image-1, b) input image-2, c) filtered image-1, d) filtered image-2, e) segmented image-1, f) segmented image-2, g) LGBP-1, h) LGBP-2, i) SLIF-1, j) SLIF-2, k) WLD-1, l) WLD-2, m) Aphids disease image, n) Bacterial blight disease image

Figure 5 illustrates healthy and target spot. Figure 5 a) expresses input image-3, Figure 5 b) represents input image-4, Figure 5 c) specifies filtered image-3, Figure 5 d) describes filtered image-4, Figure 5 e) shows segmented image-3, Figure 5 f) elucidates segmented image-4, Figure 5 g) explicates LGBP-3, Figure 5 h) demonstrates LGBP-4, Figure 5 i) depicts SLIF-3, Figure 5 j) illustrates SLIF-4, Figure 5 k) enumerates WLD-3, Figure 5 l) expresses WLD-4, Figure 5 m) indicates healthy image, and Figure 5 n) illustrates target spot.

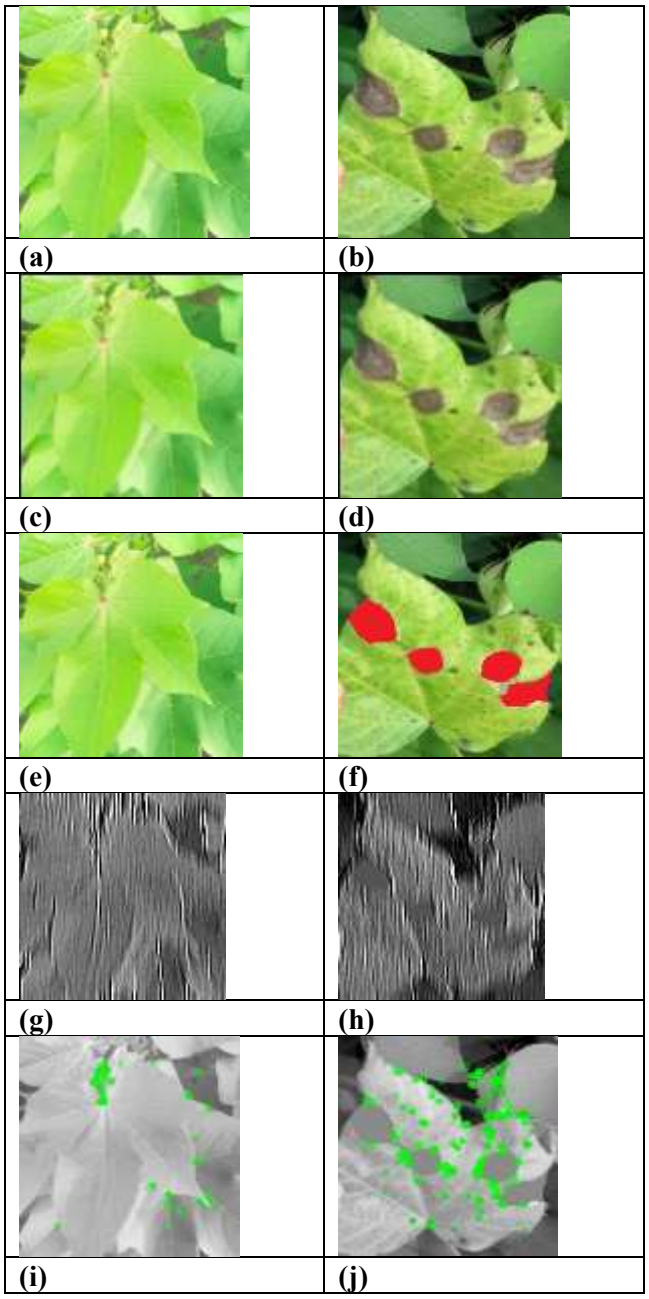

10.48047/jocaaa.2024.33.08.136

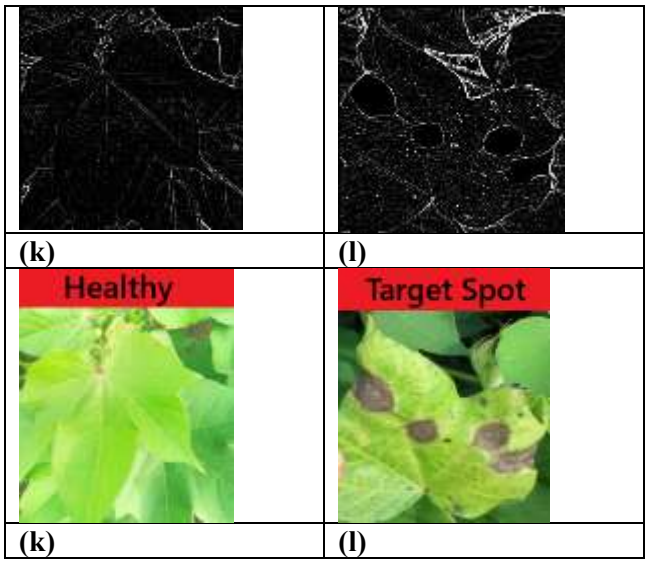

Figure 5. Image results of healthy and Target spot, a) input image-1, b) input image-2, c) filtered image-1, d) filtered image-2, e) segmented image-1, f) segmented image-2, g) LGBP-1, h) LGBP-2, i) SLIF-1, j) SLIF-2, k) WLD-1, l) WLD-2, m) healthy image, n) target spot disease image

4.4 Performance Metrics

The metrics used for assessing STCWO-EffNet_ShCNN are expressed as,

4.4.1 Accuracy

It determines the probability of correctly classified leaf samples (both diseased and healthy) to the overall samples [33], which is computed as,

$$Acc = \frac{tr_{pos} + tr_{neg}}{tr_{pos} + tr_{neg} + fal_{pos} + fal_{neg}} \tag{61}$$

Here, tr_{pos} , tr_{neg} , fal_{pos} and fal_{neg} enumerates true positive, true negative, false positive and false negative.

4.4.2 Sensitivity

It is the probability of identifying the diseased leaves accurately [33] that is expressed as,

$$sen = \frac{tr_{pos}}{tr_{pos} + fal_{neg}} \tag{62}$$

4.4.3 Specificity

It is the ratio of identifying the healthy (non-diseased) leaves accurately [33], which is enumerated as,

$$spe = \frac{tr_{neg}}{tr_{neg} + fal_{pos}} \tag{63}$$

10.48047/jocaaa.2024.33.08.136

4.5 Performance Analysis

This section evaluates STCWO-EffNet_ShCNN evaluation on basis of varying image size and K-fold.

4.5.1 Assessment of STCWO-EffNet_ShCNN using image size

Figure 6 enumerates the performance analysis of STCWO-EffNet_ShCNN based on iterations. Here, the image size is considered as $[512 \times 512]$. In Figure 6 a), the STCWO-EffNet_ShCNN evaluation with respect to accuracy is shown. The STCWO-EffNet_ShCNN in accordance with accuracy obtained 84.997%, 86.181%, 88.147%, 90.929% and 92.986% for iterations 20 to 100. Figure 6 b) illustrates STCWO-EffNet_ShCNN assessment regarding sensitivity. Here, the introduced framework with respect to sensitivity obtains 84.153%, 85.667%, 87.296%, 89.287%, and 91.637% of sensitivity for iterations of 20 to 100. In Figure 6 c), the STCWO-EffNet_ShCNN analysis in accordance with specificity is demonstrated. The STCWO-EffNet_ShCNN regarding specificity obtained 86.096%, 87.735%, 89.777%, 91.786% and 93.741% for iterations 20 to 100.

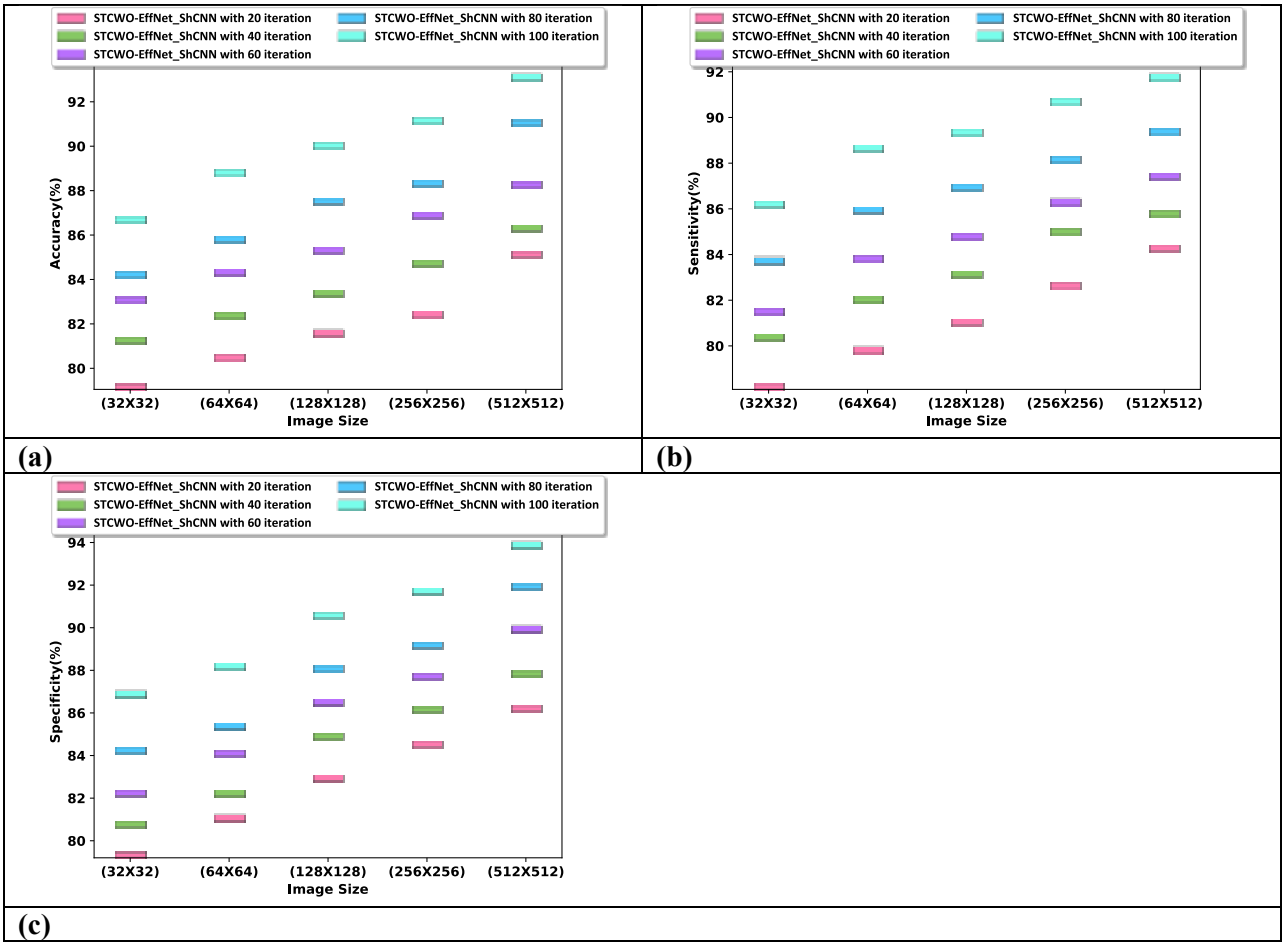

Figure 6. Assessment of STCWO-EffNet_ShCNN using image size, a) Accuracy, b) Sensitivity, c) Specificity

4.6 Comparative Methods

10.48047/jocaaa.2024.33.08.136

S-DenseNet [11], BCAEM [12], SRCNN [13], CNN [14], EffNet_ShCNN are the existing modules used to prove the efficiency of proposed STCWO-EffNet_ShCNN.

4.7 Comparative Analysis

This section demonstrates STCWO-EffNet_ShCNN analysis by altering image size and K-fold.

4.7.1 Assessment of STCWO-EffNet_ShCNN using image size

Figure 7 elucidates STCWO-EffNet_ShCNN estimation by varying image size. Here, the image size is $[512\times512]$. Figure 7 a) demonstrates the STCWO-EffNet_ShCNN evaluation in terms of accuracy. The STCWO-EffNet_ShCNN based on accuracy achieved 92.682%, while the previous techniques gained accuracy as 85.336%, 86.442%, 87.473%, 88.985% and 90.582%. While the performance improvement of STCWO-EffNet_ShCNN achieved by comparing the previous models are 7.926%, 6.733% and 5.620%, 3.989% and 2.266%. In Figure 7 b), STCWO-EffNet_ShCNN estimation with respect to sensitivity is represented. Here, the designed approach in accordance with sensitivity gained 91.744%. Meanwhile, the performance gain of STCWO-EffNet_ShCNN compared with traditional modules are 7.205%, 5.794%, 4.108%, 3.956% and 2.289%. Figure 7 c) describes the STCWO-EffNet_ShCNN evaluation based on specificity. The STCWO-EffNet_ShCNN in terms of specificity obtained 93.816%, while the traditional methods accomplished specificity of 87.295%, 88.440%, 89.554%, 90.356% and 91.060%.

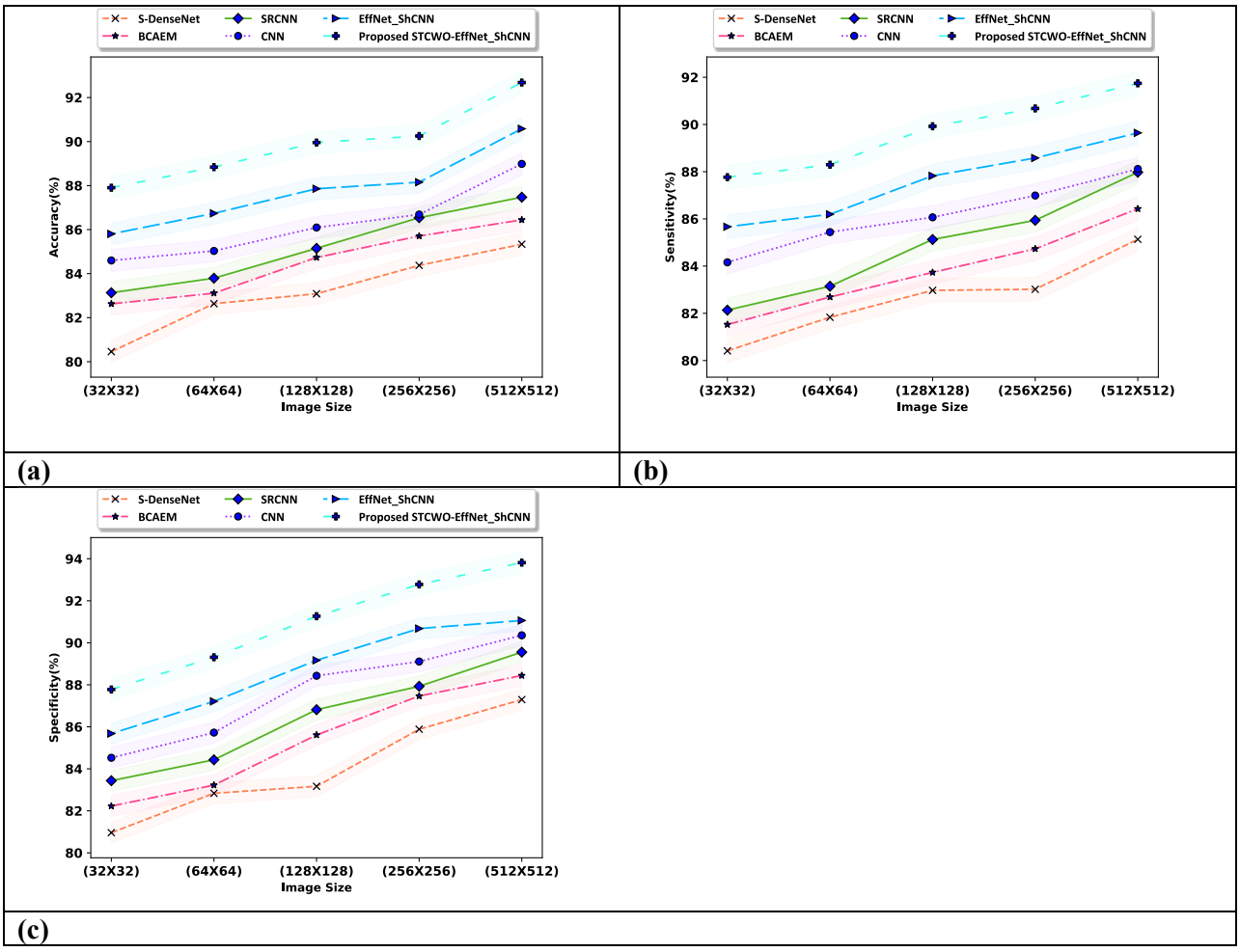

10.48047/jocaaa.2024.33.08.136

Figure 7. Estimation of STCWO-EffNet_ShCNN using image size, a) Accuracy, b) Sensitivity, c) Specificity

4.7.2 Estimation of STCWO-EffNet_ShCNN using K-fold

In Figure 8, STCWO-EffNet_ShCNN analysis by altering K-fold is elucidated. Here, K-fold is assumed as 9. Figure 8 a) illustrates STCWO-EffNet_ShCNN assessment with respect to accuracy. The STCWO-EffNet_ShCNN in terms of accuracy gained 92.745%. While comparing prior approaches, the performance enhancement of STCWO-EffNet_ShCNN achieves accuracy of 7.140%, 5.191%, 4.719%, 3.478% and 2.264%. In Figure 8 b), the STCWO-EffNet_ShCNN analysis with respect to sensitivity is represented. The STCWO-EffNet_ShCNN based on sensitivity achieved 91.320%, while the former methods obtained sensitivity as 84.649%, 85.727%, 87.756%, 88.366% and 89.220%. Figure 8 c) explicates STCWO-EffNet_ShCNN assessment in accordance of specificity. The STCWO-EffNet_ShCNN with respect to specificity acquired 93.925%. Moreover, the performance improvement of STCWO-EffNet_ShCNN compared with existing modules attains 7.133%, 6.525%, 5.436%, 4.292% and 2.952%.

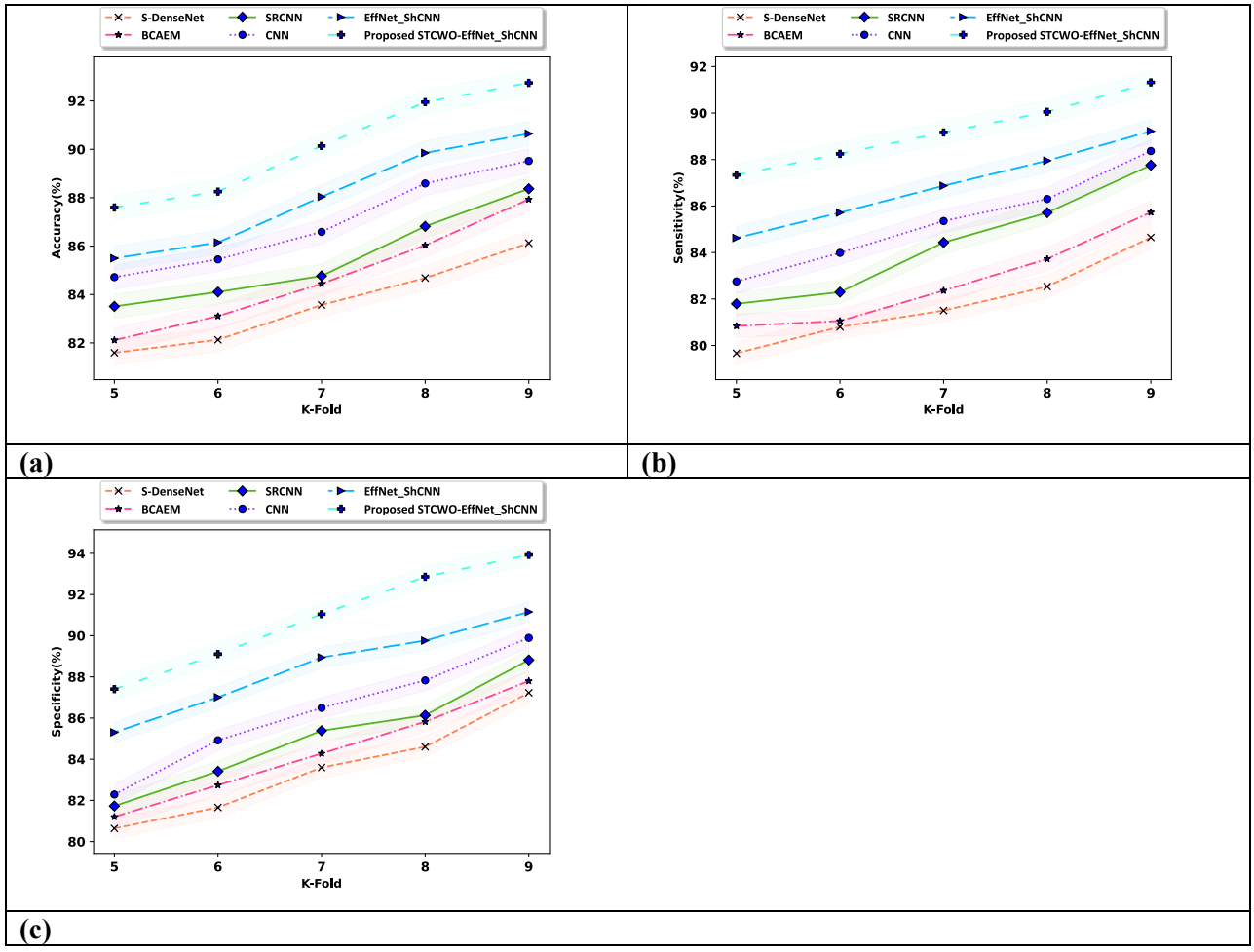

Figure 8. Assessment of STCWO-EffNet_ShCNN using image size, a) Accuracy, b) Sensitivity, c) Specificity

4.8 Comparative Discussion

10.48047/jocaaa.2024.33.08.136

Table 1 demonstrates comparative discussion of STCWO-EffNet_ShCNN. The accuracy of the STCWO-EffNet_ShCNN approach gained 92.745%, while the other methodologies obtained accuracy of 81.592%, 82.113%, 83.509%, 84.718% and 85.497%. This maximum value shows that the novel framework provides superior indication of model performance and the classes are relatively balanced. The sensitivity of the introduced approach observed 91.320%, whereas the traditional methods accomplished 84.649%, 85.727%, 87.756%, 88.366% and 89.220%. This high sensitivity value of STCWO-EffNet_ShCNN is efficient at identifying most of the actual positive cases that are significant for timely intervention and control measures in agriculture. The STCWO-EffNet_ShCNN regarding specificity acquired 93.925%, whereas preceding models obtained 87.226%, 87.797%, 88.820%, 89.894%, and 91.152%. This high specificity value shows that the novel technique reduced the risk of taking unnecessary and potentially harmful actions based on false disease predictions. This evaluation outcome reveals that the designed technique ensured that the models performed well and obtained the specific needs of agricultural diagnostics in terms of precisely identifying and managing diseases.

Table 1. Comparative Discussions

Variations	**Metrics/ Methods**	**S-Dense Net**	**BCAEM**	**SRCNN**	**CNN**	**EffNet_ShCNN**	**Proposed STCWO-EffNet_ShCNN**
Image size= $[512\times512]$	*Accuracy (%)*	85.336	86.442	87.473	88.985	90.582	92.682
	Sensitivity (%)	85.134	86.428	87.974	88.115	89.644	91.744
	Specificity (%)	87.295	88.440	89.554	90.356	91.060	93.816
K-fold=9	*Accuracy (%)*	86.123	87.931	88.368	89.519	90.645	**92.745**
	Sensitivity (%)	84.649	85.727	87.756	88.366	89.220	**91.320**
	Specificity (%)	87.226	87.797	88.820	89.894	91.152	**93.925**

5. Conclusion

Cotton is referred to as “white gold” due to its high production, where the production can be degraded by numerous diseases that impact the leaves and overall health of the plant. As a significant global source of fiber, prompt and precise detection is essential for increasing the optimal yields and maintaining crop health. When DL and ML approaches have been introduced for addressing these issues, there are still some problems in designing lightweight techniques with less parameters that might be computationally efficient for agricultural practitioners. In this exploration, STCWO-EffNet_ShCNN is introduced for classifying cotton leaf diseases. Geometric Mean Filtering is used to filter the cotton leaf image. ROSE is employed for plant region segmentation. Moreover, feature extraction is performed using segmented image. At last, cotton leaf disease is detected by STCWO-EffNet_ShCNN, which is detected into healthy and non-healthy. In classification process, when the detected image is not healthy, the cotton leaf disease is classified into aphids, bacterial blight, healthy and targeted spots using STCWO-EffNet_ShCNN. The measures used for STCWO-EffNet_ShCNN are accuracy, sensitivity and specificity that acquired 92.745%, 91.320% and 93.925%. In future, the classification results will be integrated with environmental data like humidity and temperature to enhance the prediction and understand the future disease outbreaks.

10.48047/jocaaa.2024.33.08.136

References

[1] A. J. R. R. and V. R. , "Cotton leaf disease classification using deep convolution neural network for sustainable cotton production," In 2019 IEEE international conference on clean energy and energy efficient electronics circuit for sustainable development (INCCES), 2019.

[2] S. Tripathy, "Detection of cotton leaf disease using image processing techniques," in In Journal of Physics: Conference Series, 2021.

[3] A. J. D. R. R. and V. R. , "Classification of cotton leaf disease using multi-support vector machine," in In 2019 IEEE International Conference on Intelligent Techniques in Control, Optimization and Signal Processing (INCOS), 2019.

[4] N. R. Bhimte and V. R. T. , "Diseases detection of cotton leaf spot using image processing and SVM classifier," in In 2018 Second international conference on intelligent computing and control systems (ICICCS), 2018.

[5] H. Kukadiya, N. Arora, D. Meva and S. Srivastava, "An ensemble deep learning model for automatic classification of cotton leaves diseases," Indonesian Journal of Electrical Engineering and Computer Science, vol. 33, no. 3, pp. 1942-1949, 2024.

[6] A. K. Patra and T. Gajurel, "Improved Cotton Leaf Disease Classification Using Parameter-Efficient Deep Learning Framework," arXiv preprint arXiv:2412.17587, 2024.

[7] U. Hyder and M. R. H. Talpur, "Detection of cotton leaf disease with machine learning model," Turkish Journal of Engineering, vol. 8, no. 2, pp. 380-393, 2024.

[8] J. Amin, M. A. Anjum, M. Sharif, S. Kadry and J. Kim, "Explainable neural network for classification of cotton leaf diseases," agriculture, vol. 12, no. 12, p. 2029, 2022.

[9] A. Nagarjun, N. Manju, A. A. Darem, S. Siddesha, A. E. Yahya and A. A. Alhashmi, "An Advanced Deep Learning Approach for Precision Diagnosis of Cotton Leaf Diseases: A Multifaceted Agricultural Technology Solution," Engineering, Technology & Applied Science Research, vol. 14, no. 4, pp. 15813-15820, 2024.

[10] B. N. Pandey, R. P. Singh, M. S. Pandey and S. Jain, "Cotton leaf disease classification using deep learning based novel approach," in In 2023 International conference on disruptive technologies (ICDT), 2023.

[11] X. Liang, "Few-shot cotton leaf spots disease classification based on metric learning," Plant Methods, vol. 17, pp. 1-11, 2021.

[12] M. Shao, P. He, Y. Zhang, S. Zhou, N. Zhang and J. Zhang, "Identification Method of Cotton Leaf Diseases Based on Bilinear Coordinate Attention Enhancement Module," Agronomy, vol. 13, no. 1, p. 88, 2022.

[13] S. Takkar, A. Kakran, V. Kaur, M. Rakhra, M. Sharma, P. Bangotra and N. Verma, "Recognition of Image-Based Plant Leaf Diseases Using Deep Learning Classification Models," Nature Environment

10.48047/jocaaa.2024.33.08.136

& Pollution Technology, vol. 20, 2021.

[14] A. Magsi, R. A. Shaikh, Z. A. Shar, R. H. Arain and A. A. Soomro, "A novel framework for disease severity level identification of cotton plant using machine learning techniques," Int. J. Sci. Technol. Res, vol. 10, no. 05, 2021.

[15] R. Nazeer, S. Ali, Z. Hu, G. J. Ansari, M. Al-Razgan, E. M. Awwad and Y. Y. Ghadi, "Detection of cotton leaf curl disease's susceptibility scale level based on deep learning," Journal of Cloud Computing, vol. 13, no. 1, p. 50, 2024.

[16] R. Kumar, A. Kumar, K. Bhatia, K. S. Nisar, S. S. Chouhan, P. Maratha and A. K. Tiwari, "Hybrid approach of cotton disease detection for enhanced crop health and yield," IEEE Access, 2024.

[17] Y. Shao, W. Yang, J. Wang, Z. Lu, M. Zhang and D. Chen, "Cotton Disease Recognition Method in Natural Environment Based on Convolutional Neural Network," Agriculture, vol. 14, no. 9, p. 1577, 2024.

[18] A. Shrotriya, A. K. Sharma, A. Kumarbairwa and M. R. , "Hybrid Ensemble Learning with CNN and RNN for Multimodal Cotton Plant Disease Detection," IEEE Access, 2024.

[19] "Cotton plant disease dataset," [Online]. Available: https://www.kaggle.com/datasets/dhamur/cotton-plant-disease. [Accessed April 2025].

[20] W. Yan, C. Du, Y. Wu, X. Zheng and G. Xu, "SSVEP-EEG denoising via image filtering methods," IEEE Transactions on Neural Systems and Rehabilitation Engineering, vol. 29, pp. 1634-1643, 2021.

[21] Q. Chena, Y. Chena, L. Yanga, Y. Huangd and X. Xie, "Region-based online selective examination for weakly supervised semantic segmentation," Information Fusion, vol. 107, p. 102311, 2024.

[22] G. Liu, S. Zhang and Z. Xie, "A novel infrared and visible face fusion recognition method based on non-subsampled contourlet transform," in In 2017 10th International Congress on Image and Signal Processing, BioMedical Engineering and Informatics (CISP-BMEI), 2017.

[23] F. Fausto, E. Cuevas and A. Gonzale, "A new descriptor for image matching based on bionic principles," Pattern Analysis and Applications, vol. 20, pp. 1245-1259, 2017.

[24] A. Banerjee, N. Das and K. C. S. , "Weber local descriptor for image analysis and recognition: a survey," The Visual Computer, pp. 1-23, 2022.

[25] S. M. S. K. N. and T. B. V. , "Recognition of diseases in paddy leaves using knn classifier," in In 2017 2nd International Conference for Convergence in Technology (I2CT) , 2017.

[26] S. R. and D. V. , "Recognition and classification of paddy leaf diseases using Optimized Deep Neural network with Jaya algorithm," Information processing in agriculture, vol. 7, no. 2, pp. 249-260, 2020.

[27] K. Huang, X. Liu, S. Fu, D. Guo and M. Xu, "A lightweight privacy-preserving CNN feature extraction framework for mobile sensing," IEEE Transactions on Dependable and Secure Computing, vol. 18, no. 3, pp. 1441-1455, 2019.

10.48047/jocaaa.2024.33.08.136

[28] H. Alhichri, A. S. Alswayed, Y. Bazi, N. Ammour and N. A. Alajlan, "Classification of remote sensing images using EfficientNet-B3 CNN model with attention," IEEE access, pp. 14078-14094, 2021.

[29] H. Ishibuchi, K. Nozaki, N. Yamamoto and H. Tanaka, "Construction of fuzzy classification systems with rectangular fuzzy rules using genetic algorithms," Fuzzy sets and systems, vol. 65, no. 2-3, pp. 237-253, 1994.

[30] J. S. Ren, L. Xu, Q. Yan and W. Sun, "Shepard convolutional neural networks," Advances in neural information processing systems, vol. 28, 2015.

[31] P. Trojovsky, M. Dehghani and P. Hanus, "Siberian tiger optimization: A new bio-inspired metaheuristic algorithm for solving engineering optimization problems," eee Access, vol. 10, pp. 132396-132431, 2022.

[32] S. Alomari, K. Kaabneh, I. AbuFalahah, S. Gochhait, I. Leonova, Z. Montazeri, M. Dehghani and K. Eguchi, "Carpet Weaver Optimization: A Novel Simple and Effective Human-Inspired Metaheuristic Algorithm," International Journal of Intelligent Engineering & Systems, vol. 17, no. 4, 2024.

[33] M. Sharma, M. N. Kumar and P. Kumar, "Badminton match outcome prediction model using Naïve Bayes and Feature Weighting technique," Journal of Ambient Intelligence and Humanized Computing, vol. 12, pp. 8441-8455, 2021.